curred. This phenomenon has been described in rats, which, like mice, normally ovulate spontaneously and exhibit regular estrous cyclicity, but which, when maintained in conditions of constant light for prolonged periods, enter persistent vaginal estrus (*18*). Such rats may ovulate "reflexively" in response to copulation (*19*). The neural pathway involved in reflex ovulation has not been fully defined, but the response is abolished by pelvic neurotomy (*20*). The female mouse is less affected by conditions of constant light (*21*), since after 120 days in constant light only 12.5 percent of female mice exhibited persistent vaginal cornification compared to 80 percent of rats housed in the same chamber. In fact, despite having more variable cycle lengths than rats, young adult mice do not show prolonged periods of persistent estrus, although with aging (13 to 16 months), such episodes begin to appear (*22*). Thus, although estrous cyclicity in mice is affected by male odor (*17*), there have not, to our knowledge, been any previous reports in mice of reflex ovulation within hours of the stimulus.

It is important to determine whether any hypogonadal mice with POA grafts are capable of normal estrous cyclicity. Such capability may depend on the establishment of certain critical neural connections between the host brain and the transplant. Various peptide and nonpeptide transmitters have been implicated in the regulation of GnRH-containing neurons (*23*), but the essential interactions are unknown. Nevertheless, our present understanding of the control of ovulation indicates that reflex ovulation is also a neurally mediated event, although the final pathway is not yet defined. In at least seven hypogonadal females with fetal POA grafts, neuronal connections necessary to permit ovulation were established.

MARIE J. GIBSON
DOROTHY T. KRIEGER
Department of Medicine, Mount Sinai School of Medicine, New York 10029
HARRY M. CHARLTON
Department of Human Anatomy, Oxford University, Oxford, United Kingdom OX1 3QX
EARL A. ZIMMERMAN
ANN-JUDITH SILVERMAN
Departments of Neurology and *Anatomy, College of Physicians and Surgeons, Columbia University, New York 10032*
MARK J. PERLOW
Augustana Hospital and Neurology Service, Veterans Administration, Chicago, Illinois 60680

References and Notes

1. B. M. Cattanach, C. A. Iddon, H. M. Charlton, S. A. Chiappa, G. Fink, *Nature (London)* **269**, 338 (1977).
2. R. W. Ewer, *J. Clin. Endocrinol. Metab.* **28**, 783 (1968).
3. H. M. Charlton *et al.*, *Endocrinology* **113**, 535 (1983).
4. Y. Yoshimoto, K. Moridera, H. Imura, *N. Engl. J. Med.* **292**, 242 (1975); C. H. Mortimer, A. S. McNeilly, R. A. Fisher, M. A. F. Murray, G. M. Besser, *Br. Med. J.* **4**, 617 (1974).
5. D. Gash and J. R. Sladek, Jr., *Peptides* **1**, 11 (1980); M. J. Perlow *et al.*, *Science* **204**, 643 (1979); W. C. Low *et al.*, *Nature (London)* **300**, 260 (1982).
6. D. T. Krieger *et al.*, *Nature (London)* **298**, 468 (1982).
7. M. J. Gibson *et al.*, *Endocrinology* **114**, 1938 (1984).
8. Tissue from the ventral brains of 16- to 18-day fetuses was dissected just posterior to the bifurcation of the anterior cerebral artery. The block of tissue included the POA and was approximately 1.0 mm wide by 0.5 mm deep by 0.7 mm anterior to posterior. Segments from two fetuses were pooled for each graft in a drop of 0.9 percent sterile saline. Tissue was injected stereotaxically (*6*) with a modified 22-gauge needle into the anterior third ventricle of anesthetized mice 2½ months of age.
9. G. Raisman and P. M. Field, *Brain Res.* **54**, 1 (1973); R. A. Gorski, J. H. Gordon, J. E. Shryne, A. M. Southam, *ibid.* **148**, 333 (1978).
10. Radioimmunoassay of LH and FSH was performed with kits for rat FSH and LH (provided by the National Institute of Child Health and Human Development); rLH–RP-2 and rFSH–RP-2 were used as reference standards. Because these reference preparations are more potent than the respective RP-1's previously used, the NICHD advises that with RP2 the values for LH will be 61 times lower than formerly reported, while those for FSH will be 45 times lower.
11. After perfusing four animals intracardially with saline (20 to 30 ml) and Zamboni's fixative (*12*), we removed their brains, cut them into blocks (*6*), and immersed them in Zamboni's overnight. The region from the septal nuclei to the mammillary bodies was then cut into 50- to 60-μm sections on a Vibratome. The sections were washed and incubated sequentially in 0.1*M* sodium periodate (10 minutes), 0.1 percent sodium borohydride (10 minutes), and antiserum to luteinizing hormone–releasing hormone (LR-1, a gift of R. Benoit) diluted 1:10,000 and containing 0.02 percent saponin (48 to 72 hours), a biotinylated goat antibody to rabbit serum (60 minutes), and a complex of avidin, biotin, and horseradish peroxidase (60 minutes) (Vectastain). The horseradish peroxidase was visualized with 3,3′-diaminobenzidine and the hydrogen peroxide was generated with glucose oxidase; this reaction was allowed to continue for 30 to 60 minutes. All reactions were carried out at room temperature except for the exposure to primary antiserum, which took place at 4°C. After their exposure to diaminobenzidine the sections were washed, mounted on glass slides, dehydrated, and covered with cover slips.
12. The brains were cut into blocks (*6*), immersed in Bouin's fixative overnight, dehydrated in graded alcohols, embedded in paraffin, cut serially in the coronal plane, and placed on glass slides. Sections were deparaffinized and every tenth section was stained with cresyl violet; intervening sections were reacted with rabbit antiserum to GnRH diluted 1:10,000 for 48 hours and then exposed to avidin-biotin-peroxidase complex and diaminobenzidine to produce reaction products [(*6*); S. M. Hsu, L. Raine, H. Fanger, *J. Histochem. Cytochem.* **29**, 577 (1981)].
13. J. W. Witkin, C. M. Paden, A. J. Silverman, *Neuroendocrinology* **35**, 429 (1982).
14. K. M. Knigge and A. J. Silverman, in *Handbook of Physiology*, S. R. Geiger, Ed. (Academic Press, New York, 1974), pp. 1–32.
15. Y. Sakuma and D. W. Pfaff, *Nature (London)* **283**, 566 (1980); *Neuroendocrinology* **36**, 218 (1983).
16. C. A. Barraclough and J. H. Leathem, *Proc. Soc. Exp. Biol. Med.* **85**, 673 (1954); R. A. Gorski, *Endocrinology* **82**, 1001 (1968).
17. W. K. Whitten, *J. Endocrinol.* **13**, 399 (1956).
18. L. G. Browman, *J. Exp. Zool.* **75**, 375 (1937); J. W. Everitt, *Endocrinology* **25**, 123 (1939).
19. K. Brown-Grant, J. M. Davidson, F. Greig, *J. Endocrinol.* **57**, 7 (1973); K. Brown-Grant, *Horm. Behav.* **8**, 62 (1977).
20. M. X. Zarrow and J. H. Clark, *J. Endocrinol.* **40**, 343 (1968).
21. W. Jochle, *Ann. N.Y. Acad. Sci.* **117**, 88 (1964); C. S. Campbell, K. D. Ryan, N. B. Schwartz, *Biol. Reprod.* **14**, 292 (1976).
22. J. F. Nelson, L. S. Felicio, P. K. Randall, C. Sims, C. E. Finch, *ibid.* **27**, 327 (1982).
23. G. Fink, H. F. Stanley, A. G. Watts, in *Brain Peptides*, D. T. Krieger, M. J. Brownstein, J. B. Martin, Eds. (Wiley, New York, 1983), p. 413.
24. This work was supported in part by NIH grant 1RO1NS20335.

13 April 1984; accepted 14 June 1984

The Goldfish Ear Codes the Axis of Acoustic Particle Motion in Three Dimensions

Abstract. *Auditory and vestibular nerve fibers of the goldfish are strongly directionally sensitive to whole-body acceleration at audio frequencies. The three-dimensional pattern of sensitivity shows that input from a receptor ensemble (hair cells) is essentially equivalent to that expected from a single hair cell having a given three-dimensional orientation of best sensitivity. Fibers from the sacculus, lagena, and utriculus differ with respect to distributions of directional orientation, but are similar in best threshold (less than 1 nanometer, root mean square, at 140 hertz). In combination with other mechanisms for detection of sound pressure, this directionality is a likely basis for directional hearing in fishes, and it could allow the determination of underwater acoustic intensity.*

Otolith organs of the ear respond to accelerations resulting from gravity and movements in space and generally operate on the principle of an accelerometer (*1*). In terrestrial animals, the saccular and utricular organs are part of the vestibular system, and their function is usually restricted to frequencies below 10 Hz (*2*). In fishes, however, the otolith organs may have auditory functions as well and a usable frequency range exceeding 1 kHz in some species (*3, 4*). A general route of sound to the ear in all fishes operates in an essentially "vestibular" fashion: acoustic particle movement engages the animal's body, and the mass-loaded otolithic ears function essentially as inertial devices in sensing this motion (*5*).

The sensing elements are the hair

cells, typical of all vertebrate octavolateralis systems. Hair cells are directional in that motion along an axis perpendicular to the cilia, and pointing across the cell to the kinocilium, is excitatory. Motion at 90° to this has no effect (*6, 6a*). Each otolith organ has a macula, over which the hair cells are arranged with axes of best sensitivity pointing in various directions (*7*).

Behavioral evidence demonstrates far-field sound source localization (in both the horizontal and vertical planes) in several fish species (*8*). Recent theoretical work on this question suggests that the first step in source localization is to estimate the axis of acoustic particle motion using arrays of directionally sensitive detectors (*9*).

This study was designed to investigate how the axis of particle motion impinging on the goldfish at audio frequencies is coded in fibers of the eighth nerve innervating the three otolith organs. A stimulation system that produces whole-body acceleration along any axis in space made it possible to describe directional receptive fields for auditory and vestibular neurons in three dimensions. The results are consistent with the notion that each nerve fiber receives input from a group of hair cells that is essentially equivalent to a single hair cell's having a certain three-dimensional orientation of its best-sensitivity axis.

Extracellular recordings were made of single units from visually identified saccular, lagenar, and utricular branches of the goldfish eighth nerve (*10*). Animals were anesthesized, immobilized, and connected to a respirator (*11*) in a water-filled aluminum cylindrical dish (*12*). The head was clamped to a metal respirator tube (*13*) rigidly attached to the cylinder wall.

Stimuli were whole-body linear accelerations of the dish. These were produced in the horizontal plane with two pairs of vibrators oriented 90° to one another, each pair operating in a push-pull manner. Vertical motion was produced by a larger shaker supporting the dish (*14*). Acceleration along any axis was produced by determining the appropriate phase and amplitudes for sinusoidal inputs to the three vibrator channels (*15*). Three-dimensional dish motion was reconstructed with three calibrated accelerometers oriented along orthogonal axes (*16*). Thirty-six motional axes were used: 12 axes spaced at 15° intervals in each of the animal's horizontal, sagittal, and frontal planes (*17*).

A cell's "threshold" for 140-Hz motion was determined for each axis through the use of a tracking procedure with a phase-locking criterion (*18*). The threshold acceleration, the angle of the motional axis in the given plane (obtained from accelerometer measurements during calibration), and the phase angle of the synchronized neural response (*19*) were obtained for each axis.

Figure 1 shows acceleration threshold versus axis angle in each plane for a representative saccular unit. As for each of the 136 cells studied, thresholds could be best fit with a linear function, the threshold line (*20*). This line is summarized by the magnitude of the normal vector from the origin to the threshold line (best sensitivity for the plane), and the polar angle of this vector (the axis of best sensitivity). Data from each of three planes defined a three-dimensional threshold plane (*21*) for each cell. Spherical coordinates of a vector normal to the plane (from the origin to the plane) characterized the three-dimensional sensitivity for each cell (*22*).

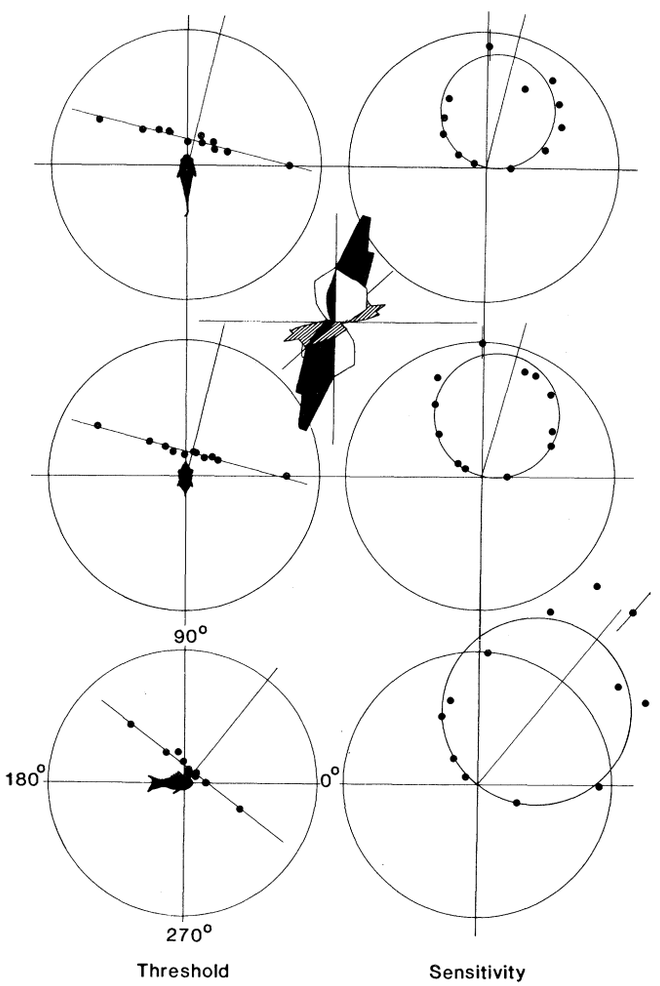

Fig. 1. Polar plots of the acceleration thresholds (left) and acceleration sensitivity (right) for saccular unit 7.6; spontaneous rate = 153 impulses per second. At the top is the *x-y* plane, looking down on the fish. The middle shows the *x-z* plane, looking at the fish from behind. The bottom is the *y-z* plane, looking at the fish from its right. For each plane, the highest threshold was not plotted since it fell well outside the limits of the figure. The perpendiculars to the threshold lines define the angle of lowest threshold projected onto the given plane. The distance along this line from the origin to the threshold line defines the magnitude of the lowest threshold. On the right, the data were plotted as the reciprocal of acceleration threshold, and the best fitting circles derived from the threshold lines. The bars on the most sensitive points indicate ±1 dB. Also shown is a three-dimensional representation of this cell's directional sensitivity, as if the fish were viewed from the back, from the right, and from above. The black plane is sagittal (*y-z*), the white is frontal (*x-z*, on the plane of the paper), and the striped is horizontal (*x-y*). The spherical coordinates of the cell's best direction vector are 76° azimuth, 42° elevation, and best sensitivity is −149 dB with reference to 1 m (root mean square).

That planar projections of a cell's thresholds could be well fit with straight lines is interpreted as follows. The input to a neuron has a single axis of excitation (the lowest threshold vectors of Fig. 1), and the axis of any motional input can be analyzed as having one component along this axis, and one at 90°. The cell will produce a threshold response to any input only when the component of motion along the "best axis" reaches a certain magnitude. This is equivalent to the description of a hair cell's sensitivity function as proportional to the cosine of the angle of displacement relative to the cell's axis of best sensitivity (*6a*). Figure 1 also shows sensitivity functions for the same cell. The same circular shape can be seen in each plane, showing that the sensitivity solid is a sphere, tangent at the origin and with the axis of best sensitivity passing through its center. This is consistent for all cells studied and suggests that the input to each neuron is equivalent to a single hair cell's having a given orientation.

Figure 2 shows that each otolith organ has a characteristic directional response pattern. The distribution for the saccule shows a tight cluster; all neurons essentially "look" along the same axis. This corresponds to anatomical observations that all cells of the goldfish saccule are oriented along the same axis (*23*). The utricular distribution is distinct; most cells are fanned out at a wide range of azimuths in the horizontal plane. This corresponds to the nearly horizontal orientation of the utricular macula (but with some curvature out of the horizontal), and the wide distribution of hair cell orientations characteristic of the utricle (*23*). The lagenar cells show a less distinct distribution but tend to fall along a roughly vertical plane with an azimuth of about 60°. Lagenar cells also tend to cluster more vertically and show overlap with both saccular and utricular cells. This is consistent with the nearly vertical orientation of the lagena and with a considerable fanning out of hair cell orientations over the macula.

These results show that each otolith organ is "looking" at different classes of directional input. The axis of particle motion for an acoustic plane wave could be reconstructed by the brain if each of these inputs were labeled according to their axes of best sensitivity. This may be the basis for a place principle of directional coding in the goldfish auditory system.

The sensitivity of cells varied widely, with the most sensitive responding robustly to root-mean-square displacements as small as 100 pm and the least sensitive to displacements above 1 μm. Generally, those cells with greatest spontaneous activity were more sensitive, and the lagenar cells were on the average slightly more sensitive than those of the saccule and utricle. At 140 Hz, 100-pm displacements would accompany a far-field sound pressure level of about 1 dyne/cm. This pressure level is about 25 dB above absolute threshold (in quiet) for the goldfish and most other species, and therefore falls at the lower range of sound levels which would transmit biologically relevant information under "real world" conditions.

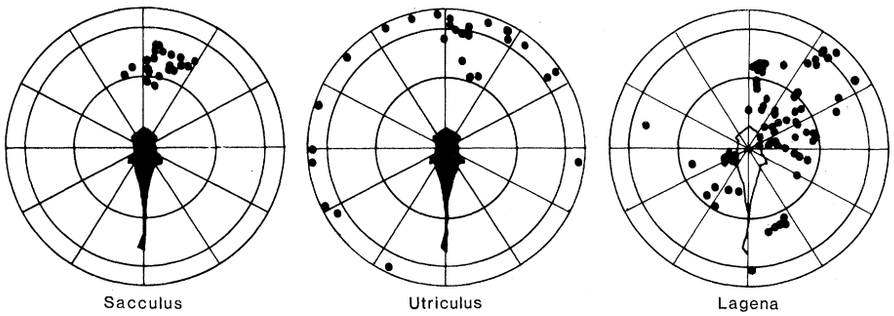

Fig. 2. Distributions of best direction vectors for 135 units of the saccular (n = 22), lagenar (n = 85), and utricular (n = 29) branches of the eighth nerve. The view is down onto a northern hemisphere with the fish's ears at the globe's center. The symbols locate the points at which best-direction axes penetrate the northern hemisphere. Sensitivity is not represented. Present data do not allow a determination of whether northward or southward motion from the globe's center is excitatory.

Each otolith organ is characterized by hair cells of opposing orientation—groups sensitive along the same axis but pointing in opposite directions. I had expected to see a correlate for this in the phase angles at which synchronized responses occurred, but found none. Although each cell was internally consistent in terms of its response phase for each of the 36 stimuli, the across-fiber distribution of phase angles was broad and showed no tendency to be bimodal. This variation may reflect a complex filtering operation between mechanical input and the neural response, which differs for each cell. However, this operation does not produce a complex frequency-response function; the acceleration tuning curves for these cells tend to be broad and low-pass.

It is now clear that the otolithic ears of the goldfish (and other fish species) code the sound-pressure waveform (through input to the saccule from the swim bladder) and the particle-motion waveform (through the direct inertial route used in these experiments) through directionally sensitive receptors. These are the essential features of a detection system that, after appropriate central processing, is capable of directional hearing (*24*), range determination (*25*), and impedance characterization. In addition, these features make possible the measurement of underwater acoustic intensity and the imaging of acoustic sources.

RICHARD R. FAY
Parmly Hearing Institute
and *Department of Psychology,*
Loyola University of Chicago,
Chicago, Illinois 60626

References and Notes

1. H. de Vries, *Acta Oto-Laryngol.* **38**, 262 (1950).
2. C. Fernandez and J. M. Goldberg, *J. Neurophysiol.* **39**, 996 (1976).
3. R. R. Fay and A. N. Popper, *J. Exp. Biol.* **61**, 243 (1974); *ibid.* **62**, 379 (1975).
4. K. von Frisch, *Z. Vergl. Physiol.* **2**, 703 (1938); D. Poggendorf, *ibid.* **34**, 222 (1952); R. R. Fay, C. M. Hillery, K. Bolan, *Comp. Biochem. Physiol.* **71A**, 181 (1982).
5. S. Dijkgraaf, *Proc. R. Soc. London Ser. B* **152**, 51 (1960); R. R. Fay, in *Hearing and Sound Communication in Fishes*, W. Tavolga, A. Popper, R. Fay, Eds. (Springer, New York, 1981), pp. 189–219; A. D. Hawkins and K. Horner, *ibid.*, pp. 311–327; R. R. Fay and A. N. Popper, *J. Exp. Biol.* **62**, 379 (1975); R. R. Fay and L. W. Olsho, *Comp. Biochem. Physiol.* **62A**, 377 (1979).
6. A. J. Hudspeth and D. P. Corey, *Proc. Natl. Acad. Sci. U.S.A.* **74**, 2407 (1977).
6a. A. Flock, *Acta Oto-Laryngol. Suppl.* **199**, 1 (1965).
7. A. N. Popper, *J. Morphol.* **153**, 397 (1977).
8. Behavioral experiments are summarized in A. Schuijf and R. Buwalda, in *Comparative Studies of Hearing in Vertebrates*, A. Popper and R. Fay, Eds. (Springer, New York, 1980), pp. 43–77.
9. A. Schuijf, in *Hearing and Sound Communication in Fishes*, W. Tavolga, A. N. Popper, R. R. Fay, Eds. (Springer, New York, 1981), pp. 267–310.
10. Electrodes were KCl-filled pipettes, 20 to 60 megohms.
11. Animals were initially anesthetized with ethyl *m*-aminobenzoate methanesulfonate (diluted with water to a ratio of 1:5000) immobilized with Flaxedil (1 μg per gram of body weight) and connected to a respirator with aged aerated tap water circulating at a rate of 0.25 liter/min.
12. The cylinder was machined aluminum, 16.5 cm in diameter, 6 cm high, with a wall thickness of 0.65 cm.
13. The head holder has been described [R. R. Fay, *J. Acoust. Soc. Am.* **63**, 136 (1978)].
14. The horizontal shakers were B&K 4810, and the vertical shaker was a B&K 4809.
15. Signals were synthesized on a D.E.C. LSI-11 system, readout of three 12-bit digital-analog channels at 0.25 msec per point, low-pass filtered at 2 kHz, attenuated by Charybdis attenuators, amplified by Crown Powerline-2 amplifiers, and attenuated by 20 dB. The amplitudes and phases required to produce a given axis of motion were determined empirically for each of the 36 stimuli, and the parameters were stored for use by the data-collection program.
16. Three PCB 303A accelerometers were attached to the cylinder to measure motion along the axes

of the three shaker channels. Their outputs were recorded and averaged over 32 cycles for each of the 36 stimuli used. The amplitudes and axis angles of the stimuli were calculated from these waveforms.
17. An optical displacement transducer (MTI KD320 Fotonic sensor) was used to confirm that the cylinder moved in phase and as a rigid body at 140 Hz and that the fish's skull, clamped to the cylinder wall, moved at the same phase and amplitude.
18. All data were collected in the form of period histograms for stimulus durations of 1 second. For cells with low spontaneous rates the tracking variable was the first harmonic discrete Fourier transform of the period histogram, R_1, with the criterion set at 80 spikes per second [D. O. Kim and C. Molnar, *J. Neurophysiol.* **52**, 16 (1979)]. For spontaneous cells, the tracking variable was the coefficient of synchronization (R_1 normalized to spike rate), with a criterion equal to 0.5. The threshold was tracked as follows. A stimulus was presented at an intermediate attenuation value and increased or decreased in 10-dB steps until the criterion response was bracketed. A preliminary threshold was then estimated by linear interpolation. Stimuli were then presented 3 dB above and 3 dB below the threshold estimate, and a final threshold estimated from these two points by linear interpolation (or extrapolation).
19. The phase angle of the period histogram is essentially the location in the cycle of the peak spike rate.
20. The threshold points of Fig. 1 were converted to Cartesian coordinates and a least-squares method used to find the best fitting line, omitting the highest threshold from the analysis.
21. Each best-fitting threshold line has intercepts on the abscissa and ordinate. Since a line was defined in each of the *x-y*, *x-z*, and *y-z* planes, there were two estimates each of the *x*, *y*, and *z* axis intercepts. These two estimates were averaged for each of the three intercepts, and these three points were used to define the equation for the three-dimensional threshold plane.
22. Spherical coordinates consist of an azimuth (straight ahead defined as 90°), an elevation (vertical defined as 0°), and a magnitude (defined as an acceleration in decibels with reference to 1 g).
23. C. Platt, *J. Comp. Neurol.* **172**, 283 (1977).
24. A. Schuijf, *J. Comp. Physiol.* **98**, 307 (1975).
25. _____ and A. D. Hawkins, *Nature (London)* **302**, 143 (1983).
26. Sincere thanks are extended to D. Monitto and C. Fay of Monitor-Aerospace, Amityville, N. Y., for donating the materials and making available the considerable talents of machinists C. Johnson, R. Dopkins, and H. Wisiak in the construction of the precision-machined steel frame supporting the five vibration exciters. Thanks to P. Harder for the set of programs used in these experiments. Thanks also to J. Baumann, S. Coombs, B. Yost, and T. Dye for help and discussions. This research was supported by NSF grant BNS-8111354 and an NIH Research Career Development Award to R.F.

9 February 1984; accepted 17 May 1984

Neuroleptic-Induced Decrease in Plasma Homovanillic Acid and Antipsychotic Activity in Schizophrenic Patients

Abstract. *Plasma-free homovanillic acid, a major metabolite of dopamine, was measured in chronically ill schizophrenic patients both before and during treatment with the antipsychotic phenothiazine, fluphenazine. Neuroleptic treatment was associated with a significant time-dependent decrease in plasma homovanillic acid from pretreatment values, which were significantly elevated when compared with those of age- and sex-matched healthy control subjects. Further, both the absolute concentrations as well as the neuroleptic-induced reductions in plasma homovanillic acid determined over 5 weeks of neuroleptic treatment were statistically significantly correlated with ratings of psychosis and improvement in psychosis, respectively. These findings suggest that the delayed effects of neuroleptic agents on presynaptic dopamine activity may more closely parallel their therapeutic actions than do their immediate effects in blocking postsynaptic dopamine receptors and that a decrease in dopamine "turnover" may be responsible for their antipsychotic effects.*

The dopamine hypothesis of schizophrenia proposes that a functional overactivity of central dopaminergic neurotransmission underlies the development of psychotic symptoms (*1*). The evidence for this hypothesis derives principally from pharmacological studies in animals, in which neuroleptics (i) cause a short-term increase in dopamine turnover by blocking postsynaptic dopaminergic receptors (*2*), (ii) bind to dopaminergic receptors of the D_2 subtype with affinities that are correlated with their clinical potencies as antipsychotics (*3*), and (iii) selectively increase (on short-term administration) (*4*) and then decrease (on long-term administration) the spontaneous firing rate of dopamine-containing neurons in the substantia nigra and ventral tegmental areas of the rat (*5*). The dopamine hypothesis, however, has received only inconsistent support from clinical studies carried out in schizophrenic patients themselves, in which dopamine metabolites have been measured in body fluids such as cerebrospinal fluid (CSF) or in postmortem brain tissue (*6*). Further, administration of drugs that enhance functional dopamine activity in the brain have been reported not only to worsen schizophrenic symptoms (*7*) but in some cases to improve (*8*) them. More recently, reports of brain atrophy in some patients with schizophrenia have suggested the possibility of two forms of schizophrenia, one involving dopaminergic pathophysiology and the other structural brain damage of unknown etiology (*9, 10*).

Perhaps the most difficult observation to reconcile with the dopamine hypothesis of neuroleptic action is that short-term administration of antipsychotic drugs blocks dopamine receptors in animals including humans, whereas their therapeutic effects require more prolonged administration, usually a minimum of 3 weeks (*11*). Since there is now evidence that fluctuations in the plasma concentrations of the major dopamine metabolite homovanillic acid (HVA) parallel changes in dopamine turnover in the CNS (*12*), we carried out a longitudinal study in which we measured plasma HVA in chronically ill schizophrenic patients both before and during treatment with the potent neuroleptic, fluphenazine. We now report that fluphenazine treatment was associated with a time-dependent decrease in plasma HVA concentration from pretreatment values, which were significantly elevated when compared with age- and sex-matched normal controls. Further, the decreases in plasma HVA concentration were statistically significantly correlated with clinical improvement, indicating that the therapeutic effects of antipsychotic drugs like fluphenazine, may follow from a decrease in dopamine turnover that is secondary to dopamine receptor blockade.

Eight patients (three male, five female; age range, 20 to 29) meeting DSM III criteria (*13*) for the diagnosis of schizophrenia and free of physical illness were studied on a psychiatric research ward of the National Institute of Mental Health. After giving informed consent to participate in the study, all patients were kept on a low-monoamine, low-alcohol, and caffeine-restricted diet. Neuroleptic administration was carried out according to double-blind placebo-controlled methods. After a minimum of 14 days on placebo (mean ± standard error of the mean medication-free days; 28 ± 6 days) the antipsychotic phenothiazine, fluphenazine, was substituted and administered in doses ranging between 20 and 60 mg/day (*14*). Behavioral ratings were obtained weekly by physicians and daily by specially trained nursing staff, none of whom were aware of the medication status of the patient (*15*). Blood was collected by venipuncture in EDTA-containing tubes 3 days per week between 0730 and 0930 (*16*). After an overnight fast, patients remained on restricted activity until blood collection was complete. Plasma, obtained within 30 minutes of collection by centrifuging whole blood (800*g*, 10 minutes), was stored at −20°C. Plasma-free HVA was assayed by high pressure liquid chromatography with electrochemical detection (*17*).

Fluphenazine administration resulted in a time-dependent decrease in the plasma concentration of HVA (Fig. 1). The decrease in plasma HVA relative to pre-